From Prestimulus Alpha Oscillation to Visual-evoked Response: An Inverted-U Function and Its Attentional Modulation

Rajasimhan Rajagovindan and Mingzhou Ding

Abstract

■ Understanding the relation between prestimulus neural activity and subsequent stimulus processing has become an area of active investigation. Computational modeling, as well as in vitro and in vivo single-unit recordings in animal preparations, have explored mechanisms by which background synaptic activity can influence the responsiveness of cortical neurons to afferent input. How these mechanisms manifest in humans is not well understood. Although numerous EEG/MEG studies have considered the role of prestimulus alpha oscillations in the genesis of visual-evoked potentials, no consensus has emerged, and divergent reports continue to appear. The present work addresses this problem in three stages. First, a theoretical model was developed in which the background synaptic activity and the firing rate of a neural ensemble are related through a sigmoidal function. The derivative of this function, referred to as local gain, has an inverted-U shape and is postulated to be proportional to the trial-by-trial response evoked by a transient stimulus. Second, the theoretical model was extended to noninvasive studies of human visual processing, where the model variables are reinterpreted in terms of ongoing EEG oscillations and event-related potentials. Predictions were derived from the model and tested by recording high-density scalp EEG from healthy volunteers performing a trial-by-trial cued spatial visual attention task. Finally, enhanced stimulus processing by attention was linked to an increase in the overall slope of the sigmoidal function. The commonly observed reduction of alpha magnitude with attention was interpreted as signaling a shift of the underlying neural ensemble toward an optimal excitability state that enables the increase in global gain. ■

INTRODUCTION

Research into the neuronal mechanisms of cognition has mainly relied on stimulus-evoked responses and their modulation by brain circuits subserving higher mental functions such as attention and memory. Recent work has begun to explore how ongoing neural activity prior to stimulus onset influences stimulus processing and behavior. In human visual cortex, the relation between prestimulus alpha activity (8–12 Hz) and the subsequent ERP has been the subject of extensive investigation. The phase-reset model supposes that the ERP is generated as a result of stimulus-triggered alpha-phase realignment and predicts a positive correlation between the prestimulus alpha power and the magnitude of early visual-evoked response (Hanslmayr, Klimesch, et al., 2007; Makeig et al., 2002; see also Mazaheri & Jensen, 2006). Two lines of empirical evidence appear to be at variance with this prediction: (1) a state of low alpha is found to improve detection and discriminability of threshold-level stimuli (Romei, Rihs, Brodbeck, & Thut, 2008; Van Dijk, Schoffelen, Oostenveld, & Jensen, 2008; Hanslmayr, Aslan, et al., 2007; Romei, Brodbeck, et al., 2008; Ergenoglu et al., 2004) and (2) covert attention reduces prestimulus alpha amplitude and, at the same time, increases stimulus-evoked response (Thut, Nietzel, Brandt, & Pascual-Leone, 2006; Sauseng et al., 2005; Marrufo, Vaquero, Cardoso, & Gomez, 2001; Foxe, Simpson, & Ahlfors, 1998; Hillyard, Vogel, & Luck, 1998; Mangun, Buonocore, Girelli, & Jha, 1998; Mangun & Hillyard, 1991). The hypothesis that prestimulus alpha power should be inversely proportional to stimulus-evoked response proves to be also contradicted by studies where (1) alpha episodes over the parieto-occipital areas immediately preceding the stimulus onset enhanced the ability to detect a threshold-level visual stimuli (Babiloni, Vecchio, Bultrini, Romani, & Rossini, 2006) and (2) a higher alpha power led to a stronger evoked response (Paul, Simon, John, Richard, & Ian, 2007; Brandt & Jansen, 1991; Brandt, Jansen, & Carbonari, 1991). These divergent reports, in conjunction with recent findings in the somatosensory domain where the mu rhythm (7–13 Hz) is found to exhibit an inverted-U relationship with the ERP and behavior (Zhang & Ding, 2010; Linkenkaer-Hansen, Nikulin, Palva, Ilmoniemi, & Palva, 2004), suggest that a new assessment of the relation between alpha and visual information processing is needed. This new assessment is expected to also yield insights into the fundamental question of how brain circuits subserving cognitive operations such as attention, through modulation of baseline ongoing neural activity, achieve enhanced sensory information processing.

University of Florida

Noninvasively recorded EEG and invasively recorded local field potentials are a measure of dendritic activity in populations of neurons. Computational as well as in vitro and in vivo studies in animal preparations have shown that synaptic background activity can exert a significant influence on the responsiveness of sensory neurons to stimulus input (Haider, Duque, Hasenstaub, Yu, & McCormick, 2007; Wolfart, Debay, Le Masson, Destexhe, & Bal, 2005; McCormick et al., 2003; Chance, Abbott, & Reyes, 2002; Ho & Destexhe, 2000). Our approach to investigating the relation between prestimulus activity and stimulus-evoked response starts by considering a theoretical model in which synaptic input to a sensory neuronal ensemble comes in two forms: external stimulus (exogenous) or other brain structures (endogenous). On a moment-by-moment basis, the endogenous brain activity fluctuates randomly, and the effective processing of a stimulus depends on the state of the brain defined by these fluctuations at its onset. Supposing that, in the absence of sensory input, the firing rate of the neuronal ensemble is related to the magnitude of endogenous synaptic fluctuations through a sigmoidal function, and sensory input has an additive synaptic effect, it follows that the stimulus-evoked response corresponds to the derivative of the sigmoidal function, which is an inverted-U function of the prestimulus level of background activity. Reformulated in terms of EEG variables, where alpha oscillations and the P1 component in the ERP are treated as indices of background synaptic activity and stimulus-evoked response, the model makes a number of predictions, which were then tested by recording EEG data from human volunteers performing a trial-by-trial cued covert spatial visual attention task. Finally, a mechanism on how changes in the global state of the brain, such as selective attention, influenced the aforementioned sigmoidal curve was proposed. Through experimental data and computational modeling, the reduced magnitude and trial-to-trial variability of alpha activity are linked to an increase in cortical excitability brought about by attention, which enables an increase in the overall slope of the sigmoidal curve, hence, higher stimulus-evoked response.

METHODS

Subjects

Nineteen subjects, free from movement and neurological disorders and with normal or corrected-to-normal vision, gave written informed consent and participated in the study. Data from 12 subjects (20–31 years of age, 25.16 ± 3.5 years, 5 women and 7 men, all right-handed) were included in the analyses reported here. The remaining seven participants were excluded for a combination of three reasons: (1) poor behavioral performance (target detection rates less than 75%; 3 subjects); (2) excessive eye blinking, eye movement, and muscle activity or electrolyte bridging (3 subjects); and (3) inability to complete the experiment (1 subject).

Paradigm

The subject performed a trial-by-trial cued spatial attention experiment. The protocol was approved by the University of Florida Institutional Review Board. Seated in a dimly lit, acoustically and electrically shielded room, the subject was instructed to fixate a central cross on a VGA monitor placed approximately 85 cm from the eye. Two square boxes, each delineated by white dots placed at the four corners in the upper left visual field and in the upper right visual field, were displayed permanently on the monitor (Figure 1). Each box, centered 4.7° above the horizontal meridian and 7.2° lateral to the central fixation, subtended a visual angle of 3.35°. A trial began with the onset of a cue, which consisted of either a left or right pointing arrow of 200 msec in duration at the location of the central fixation cross, instructing the subject to deploy covert attention to the square box on the side indicated by the arrow. After a random time delay between 1800 and 2200 msec, a standard or a target stimulus of 100 msec in duration appeared either inside the attended square box (valid trial) or inside the square box on the opposite side (invalid trial). The standard stimulus was a circular checkerboard subtending a 3.3° visual angle, and the target stimulus was also a circular checkerboard, but of a slightly smaller diameter. The subject was required to press a button with their right index finger in response to the valid target stimulus and withhold response to any other stimuli. The standards appeared 80% of the time with 50% validity and the targets appeared 20% of the time with 66% validity. The interval between the cue offset of the previous trial and the cue onset of the successive trial was randomly varied between 4700 and 5700 msec. The entire experiment comprised 15 to 16 blocks of approximately 6 min each (60 trials). Breaks were given between blocks. Subjects received practice sessions of 150 trials to familiarize themselves with the task and to minimize the effect of learning.

Data Acquisition

The EEG data were recorded with a 128-channel BioSemi ActiveTwo System (www.biosemi.com) at a sampling rate of 1024 Hz. Four additional EOG electrodes were placed around the eyes to monitor eye blinks as well as horizontal and vertical eye movements. EEG and EOG data were amplified and low-pass-filtered with a cutoff frequency set at 205 Hz. The stimulus and the response were delivered and registered by a BeriSoft Experimental Run Time System (ERTS) device and by a Berisoft EXKEY microprocessor logic pad (www.berisoft.com), respectively. In addition to the attention experiment, 5 min of EEG activity during relaxed fixation were also recorded for baseline purposes.

Data Preprocessing

Analysis was performed using BESA 5.2 (www.besa.de) and custom scripts were written in MATLAB 7.4 (www.

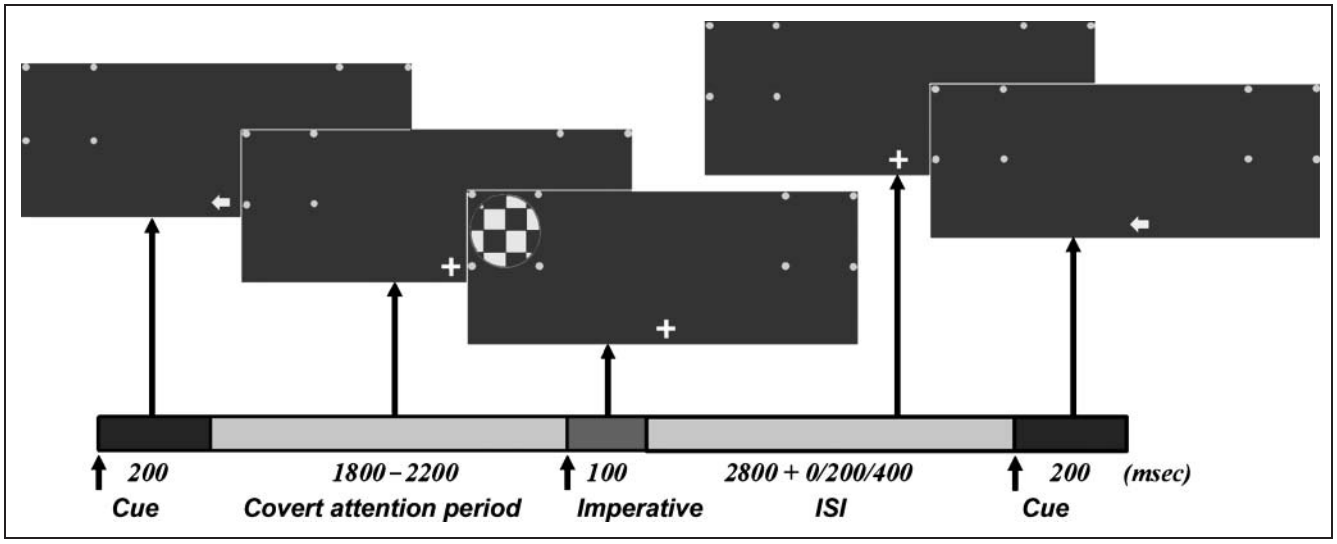

Figure 1. Experimental task. The subject was instructed to fixate a cross on the computer screen throughout the experiment. At the beginning of each trial, a cue (left/right pointing arrow) was presented at the fixation point instructing the subject to covertly attend one of two predefined locations in the upper left and upper right visual fields. After a random delay between 1800 and 2200 msec, a unilateral imperative stimulus of either target or standard type appeared at one of the two locations, and the subject indicated the occurrence of the target stimulus at the attended location by a speeded keypress response.

mathworks.com). The EEG data were filtered off-line between 1 and 83 Hz and downsampled to 250 Hz. The channels were re-referenced off-line against the average reference (Ferree, 2006; Nunez et al., 1997). Trials contaminated by any of the following factors were excluded from further analysis: (1) incorrect behavioral response; (2) excessive muscle or movement artifact; (3) eye blinks during a 150-msec period around the onset of the cue and the standard stimuli; and (4) horizontal eye movement following the cue onset and during the period −1000 to 300 msec, with 0 msec denoting the presentation of the standard stimuli. The average trial rejection rate was 24%. The remaining eye blinks were removed using the adaptive artifact correction procedure in BESA 5.2. The high rejection rate is necessary because the single-trial based analysis protocol here places stringent requirements on the quality of the EEG signal (see below). The data from the relaxed fixation condition were segmented into 300-msec-long nonoverlapping artifact-free epochs. For the spatial attention task, the continuous EEG data were epoched from −1000 to 800 msec.

Behavioral and ERP Analysis

Behavior was quantified by three measures: (1) target detection rate defined as the number of correctly identified valid targets divided by the total number of valid targets presented; (2) false alarm rates for the conditions where the participants had to withhold their responses was defined as the number of responses to (a) invalid targets, (b) valid standards, and (c) invalid standards, each divided by the total number of trials in each of these conditions; and (3) mean RT for correctly detected valid targets. The visual ERP was computed by averaging the EEG response elicited by the left and right field standard stimuli for the attend and ignore conditions. The amplitude of the ERP components was estimated using the baseline-to-peak method, where the baseline period was defined to be (−150 to 0 msec) (Luck, 2005). Paired Wilcoxon's signed-rank test was used to evaluate the statistical significance for the attentional enhancement of the ERP components over the occipital and parieto-occipital areas.

Correlation between Prestimulus Alpha Power and P1 Amplitude

A key objective of this study is to investigate how the state of the brain immediately preceding the onset of stimulus affects stimulus processing. The former is characterized by the power of the alpha oscillation (8–12 Hz) during the time period from −300 to 0 msec and the latter by the amplitude of the visually evoked P1 component (90 to 160 msec). The method for accomplishing the objective is correlation analysis and it has the following steps. (1) For each subject, between two to four neighboring electrodes overlying the occipital and parieto-occipital areas that exhibited strong P1 component were chosen for analysis in each hemisphere. (2) Prestimulus power for each of the channels was computed on a trial-by-trial basis using the multitaper spectral estimation technique (Mitra & Pesaran, 1999; Thomson, 1982), where three tapers were found to give the optimal balance between spectral smoothness and frequency resolution. This power was then averaged over the alpha frequency band and across the set of preselected channels. (3) The trials from each subject were sorted, according to the magnitude of the prestimulus alpha power determined in Step 2, from the smallest to the largest, into five groups of equal size (Rajagovindan

& Ding, 2008; Zhang, Wang, Bressler, Chen, & Ding, 2008), with 50% overlap. Each group, containing 30% of the total trials, will be henceforth referred to as a power group. (4) For every power group, the group-mean prestimulus alpha power and the baseline-to-peak group mean visually evoked P1 component were estimated for each subject. (5) To minimize the effect of intersubject variability on population averaging, the normalized P1 amplitude was obtained by dividing the evoked P1 for each power group by the largest evoked P1 component across all power groups under the attend condition for every individual subject. (6) The normalized evoked P1 component was averaged across subjects and plotted against the power group index. The relation between the two variables, reflecting prestimulus and poststimulus activities, respectively, was assessed from the scatterplot.

Characterization of Ongoing Alpha Activity

On a trial-by-trial basis, the amplitude of prestimulus alpha activity varies markedly; collectively, these amplitudes form an alpha power distribution. Past work has focused on the mean of this distribution (mean alpha power) and its modulation by attention. Here, in addition to the mean, the variance of the distribution is also given physiological importance, and compared across three conditions: attend, ignore, and relaxed fixation. For the first two conditions, the 300-msec interval prior to the onset of the standard stimulus constitutes a trial. For the relaxed fixation, continuous recordings were divided into 300-msec nonoverlapping epochs, each of which is considered a trial. The same method as that described above was used to estimate the single-trial alpha power for each hemisphere of every subject. To test the difference in alpha variance between conditions, single-trial alpha power was log-transformed to ensure an approximate normal distribution. Population differences across subjects in the magnitude of the estimates between conditions were tested for statistical significance using the paired Wilcoxon's signed-rank test.

RESULTS

The relation between prestimulus alpha oscillation and stimulus-evoked response and its attentional modulation was investigated by combining a theoretical model with EEG data from a human visual attention experiment. Below, basic experimental findings are reported first, which is followed by model analysis and test of model predictions.

Behavior

The average target detection rate across subjects was 87.3% (± 3.2% *SEM*) for attended targets appearing in the left visual field and 87.4% (± 3.7% *SEM*) for attended targets appearing in the right visual field. These results suggest that the level of task difficulty was equated between the attend-left and the attend-right conditions ($p = .8$). The average false alarm rate stemming from (1) response to the target appearing in the ignored location, (2) response to the attended standard stimulus, and (3) response to the ignored standard stimulus was 1.6%, 4.0%, and 0.2%, respectively. The mean RT was 541 msec (± 36 msec *SEM*) to attended targets appearing in the left visual field and 502 msec (± 28 msec *SEM*) to attended targets appearing in the right visual field. The difference between the two mean RTs was not statistically significant.

ERP Analysis

ERP profiles elicited by the standard stimuli under the attend and ignore conditions were compared. Waveforms from a single channel of a representative subject are shown in Figure 2A. Across subjects, the P1 component (90 to 160 msec), indexing early responses of extrastriate cortex to stimulus input, is significantly higher for the attend versus the ignore condition over the posterior electrodes ($p = .0005$, right hemisphere for attend-left vs. ignore-left and $p = .00024$, left hemisphere for attend-right vs. ignore-right; see Figure 2B). The scalp distribution of the P1 attention effect has an amplitude maximum over the lateral occipital sites contralateral to the visual field of stimulation for the attend-left condition (Figure 2C). For the attend-right condition, the pattern is more bilateral (Figure 2D), suggesting the involvement of the right hemisphere in attention to both visual fields (Heilman, Valenstein, & Watson, 2000). Attentional enhancement of the N1 component (160 to 210 msec) over the parieto-occipital areas was also observed but not pursued here.

Prestimulus Alpha Oscillations

Grand-average prestimulus power spectra from the left and right occipital areas are shown in Figure 3A and B, respectively, for three conditions: attend, ignore, and relaxed fixation. The mean spectral peak frequency averaged across subjects is 9.5 ± 0.4 Hz and no frequency difference was seen between conditions. The power of alpha activity for both the attend and ignore conditions is significantly lower than that for the fixation condition. Alpha power is further reduced with attention when the attend condition is compared to the ignore condition ($p < .002$). The scalp distribution of alpha power difference between the conditions is shown in Figure 3C–E. A hemisphere-specific modulation is seen in Figure 3C, where alpha activity was maximally suppressed over the parieto-occipital areas contralateral to the attended visual field. Specifically, for the right occipital areas, the alpha power was significantly lower when attention was directed to the left visual field compared to when attention was directed to the right visual field (ignoring the left visual field) ($p = .0034$). For the left occipital areas, the alpha band power was significantly lower when attention was directed

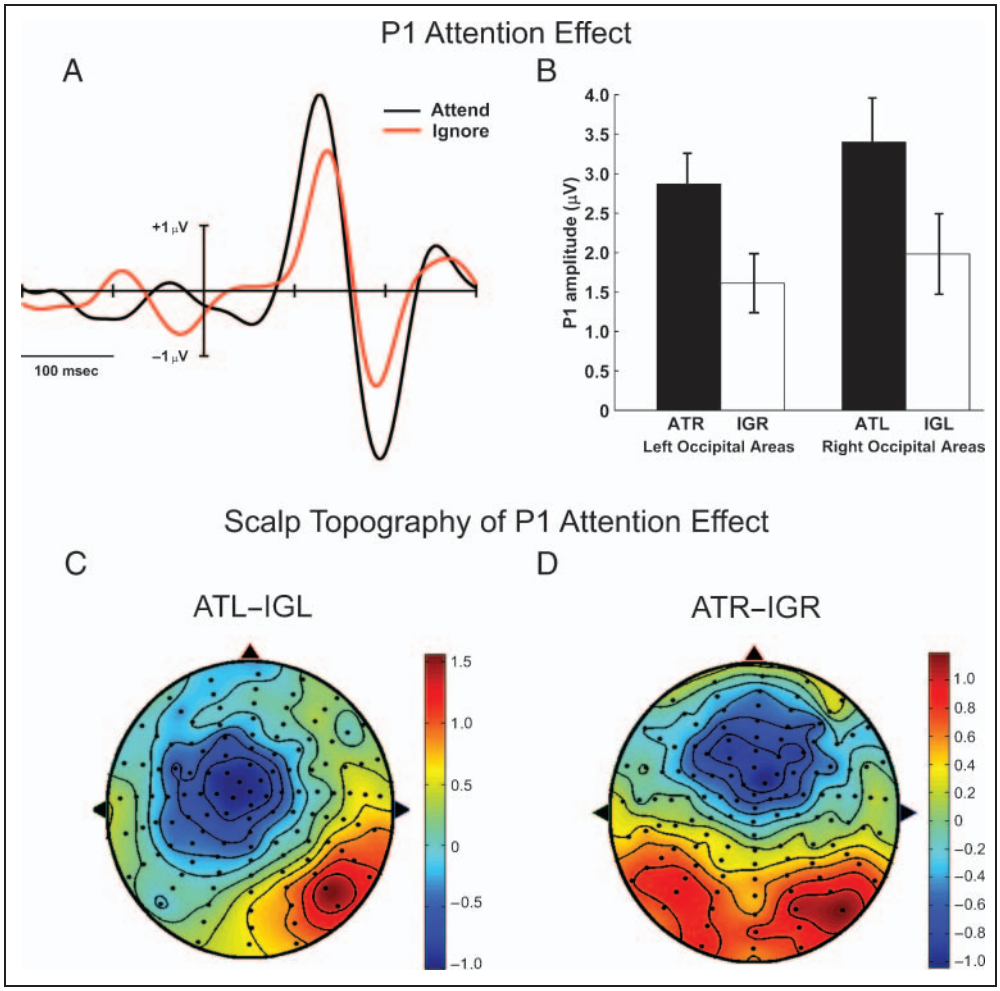

Figure 2. ERP analysis. (A) Typical waveforms of visual ERP over the parieto-occipital region contralateral to the visual field of stimulation. Attentional enhancement of P1 and N1 components is apparent. (B) P1 amplitudes to contralateral stimulation averaged over channels and subjects. (C–D) Scalp distribution of attentional enhancement of posterior P1 (shaded red) and fronto-central N1 (shaded blue) at 120 msec after presentation of the standard stimulus. ATL = attend-left; IGL = ignore-left; ATR = attend-right; IGR = ignore-right.

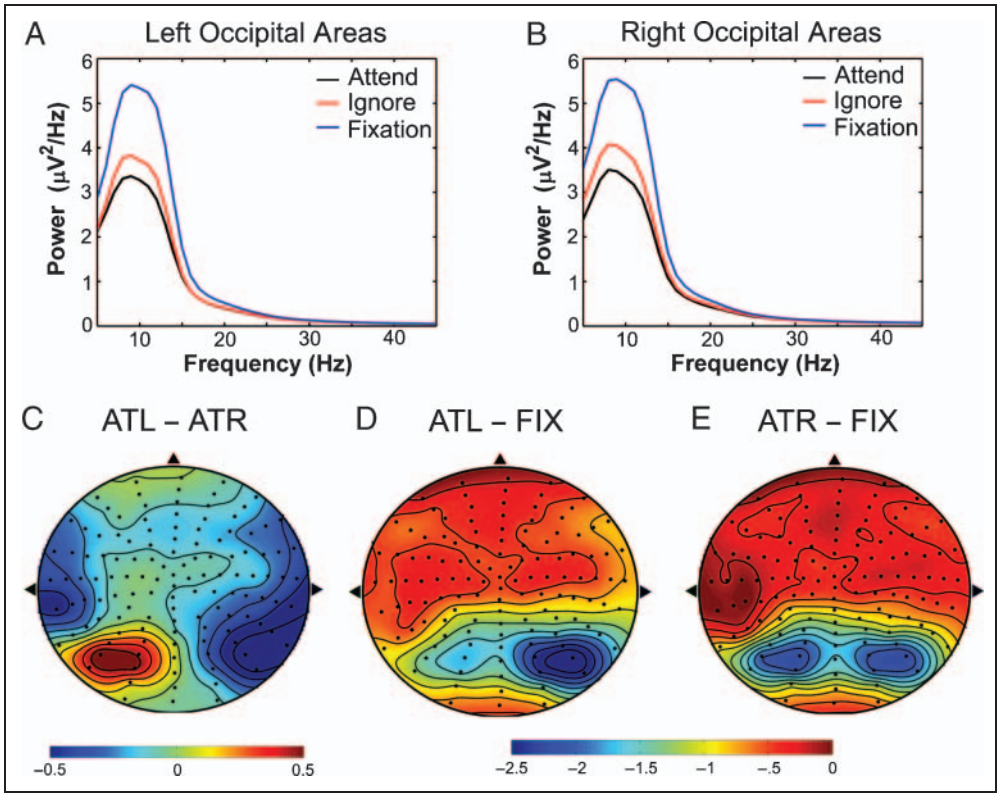

Figure 3. Attentional modulation of alpha band activity. Power spectra: (A) left parieto-occipital and (B) right parieto-occipital areas. Black: attend contralateral visual field; red: ignore contralateral visual field (attend ipsilateral visual field); blue: relaxed fixation. (C–E) Scalp topography of alpha band power differences: (C) attend-left (ATL) minus attend-right (ATR), (D) attend-left minus relaxed fixation (FIX), (E) attend-right minus relaxed fixation.

to the right visual field compared to when attention was directed to the left visual field (ignoring the right visual field) ($p = .0024$). Figure 3D and E show the comparison between task conditions and the relaxed fixation condition. Similar to the topographies of P1 modulation in Figure 2C and D, alpha power reduction is strongly contralateral for the attend-left condition, whereas it is more bilateral for the attend-right condition.

From Ongoing Activity to Evoked Response: A Model

The results above demonstrated that attention reduced alpha power prior to stimulus onset and, at the same time, enhanced the stimulus-evoked P1 component. Presumably, the prestimulus alpha power reduction contributed to the subsequently improved stimulus processing. To understand the underlying physiological mechanism, it is essential to understand the link between ongoing baseline activity and stimulus-evoked response.

The Sigmoidal Function

Consider a neuronal ensemble in sensory cortex. It is well accepted that the level of synaptic input S it receives is related to its output O measured in firing rate through a sigmoidal function $O(S)$ in Figure 4A (Destexhe, Rudolph, Fellous, & Sejnowski, 2001; Freeman, 1979). The synaptic input S can come in two forms: sensory stimulus (exogenous) or other brain structures (endogenous). Let S_N denote the amount of endogenous prestimulus background activity over a suitably defined time interval prior to stimulus onset and S_X be the amount of synaptic activity induced by the sensory input. From the schematic in Figure 4A, the stimulus-evoked response is the difference: $O(S_N + S_X) - O(S_N)$. For a constant sensory stimulus presented over repeated trials, as is the case in many cognitive neuroscience experiments, S_X is approximately the same from trial to trial over the physiological range of S. The stimulus-evoked response is then proportional to the first derivative of $O(S)$, $[O(S_N + S_X) - O(S_N)]/S_X$, which is referred to as the local gain and is a function of prestimulus synaptic activity S_N. As shown in Figure 4B, this function has an inverted-U shape, suggesting that S_N has an effective operational range, denoted by W, beyond which stimulus input evokes a negligible response. An estimate of W is provided by the variance of the distribution of the trial-by-trial values of S_N.

Model Reformulation in Terms of EEG Variables

The abscissa and ordinate of the model in Figure 4 are moment-by-moment background synaptic activity and the corresponding firing rate. Although these variables can be precisely controlled and measured in computational models and in slice preparations, they are not readily available in noninvasive human experiments. Thus, the model in Figure 4 requires reformulation to be applicable to our EEG data. First, consider the abscissa. Physiologically, EEG reflects the fluctuating extracellular dendritic currents which are, in turn, caused by synaptic input (Niedermeyer & Lopes da Silva, 1999). There is evidence that the amplitude of EEG fluctuations is proportional to the level of correlated synaptic input (Ho & Destexhe, 2000; Niedermeyer & Lopes da Silva, 1999). In this sense, the abscissa of the model in Figure 4A may be equivalently expressed by the amplitude of EEG fluctuations, which is further replaced

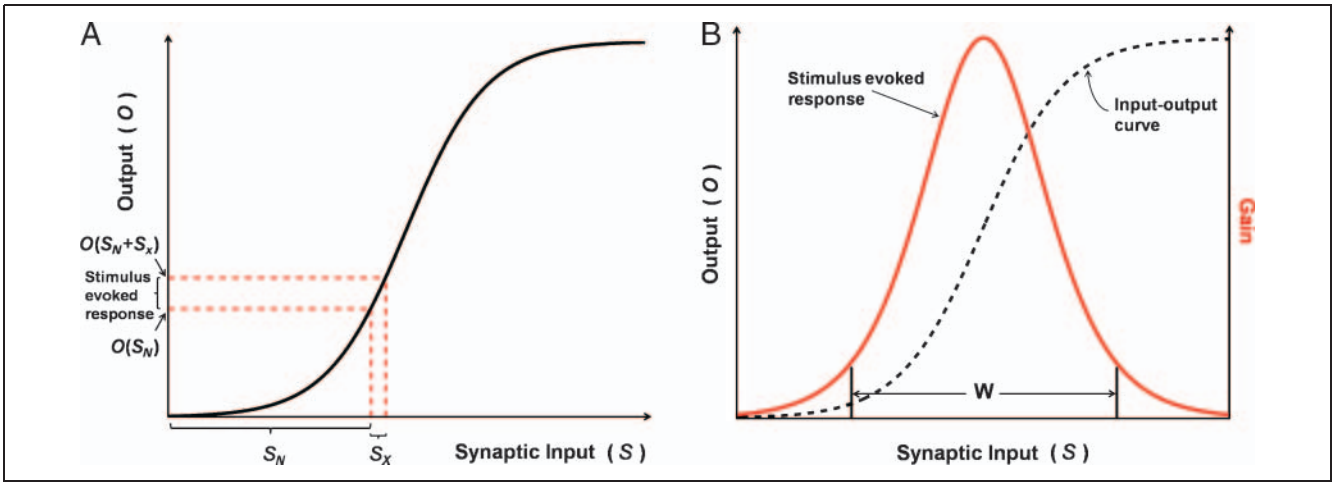

Figure 4. Schematic illustration of theoretical model. (A) For a neuronal ensemble, the spontaneous output firing rate O measured over a suitably defined time interval is a sigmoidal function of endogenous background synaptic activity level S_N measured over the same interval. Letting S_X denote stimulus-induced synaptic activity, the stimulus-evoked firing rate, $O(S_N + S_X) - O(S_N)$, is proportional to the derivative, referred to as local gain, of the sigmoidal curve, $[O(S_N + S_X) - O(S_N)]/S_X$, shown as the red curve in (B). In this model, when the stimulus is kept constant, the stimulus-evoked response is an inverted-U function of the prestimulus level of background synaptic activity. The variable W in (B) defines an effective range of prestimulus level of synaptic activity beyond which stimulus evokes a negligible response. The overall slope of the sigmoidal function over the effective range is referred to as the global gain.

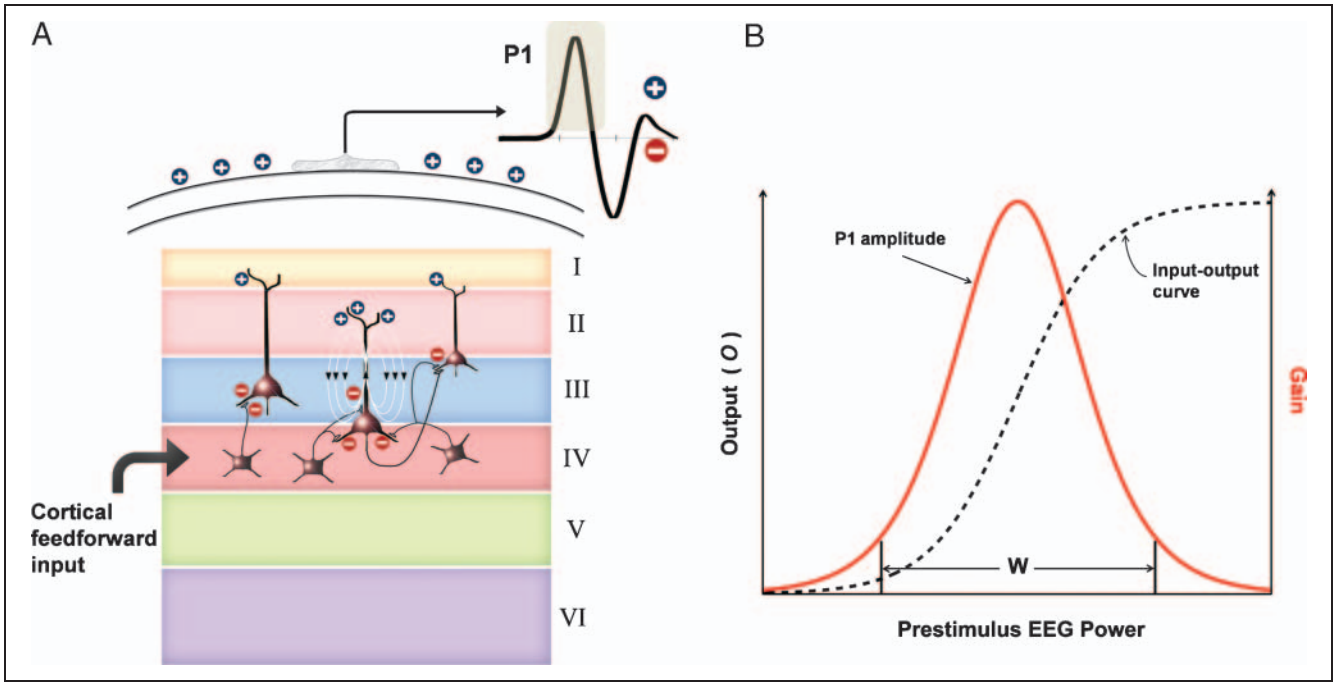

Figure 5. Model reformulation in terms of EEG variables. (A) Neural genesis of visually evoked P1. Feedforward activation of layer 4 stellate cells excites the basal dendrites of the superficial layer pyramidal cells, leading to an extracellular sink near layer 4 and an extracellular source, composed mainly of passive return current, near the cortical surface. The latter is sensed by the scalp electrode as a positive-going ERP component. (B) Reformulated model in which prestimulus EEG power in alpha band is equated with level of background synaptic activity and magnitude of P1 with intensity of stimulus-evoked response. This model predicts that the P1 amplitude is an inverted-U function of prestimulus alpha power with the variable *W* defining a range of effective operation.

here by the power of the alpha oscillations given its dominance in visual ongoing activity. Next, consider the ordinate. Firing rates are not accessible noninvasively. This means that the sigmoidal input–output curve during the ongoing brain state cannot be directly established with EEG. But the consequence of this curve on stimulus processing can be assessed via the early ERP component P1 (90 to 160 msec). Dipole modeling and imaging studies have identified ventral–lateral extrastriate cortex as the putative source for P1 (Mangun, Hopfinger, Kussmaul, Fletcher, & Heinze, 1997; Clark & Hillyard, 1996; Heinze et al., 1994). Invasive recordings in animals revealed that, upon receiving afferent input from the thalamus or lower visual areas, layer 4 stellate cells fire action potentials which excite the supragranular pyramidal cells at their basal dendrites spanning layer 3 or portion of layer 4 (Thomson & Lamy, 2007; Callaway, 1998; Mitzdorf, 1985; Gilbert & Wiesel, 1983). As illustrated in Figure 5A, this activation causes an extracellular sink in layer 3/4 and an extracellular source near the apical dendrite in layer 1/2, with the latter manifesting as a positive-going potential at nearby surface electrodes. In addition, there is evidence suggesting that the magnitude of the dendritic response, measured here by the P1 amplitude, is proportional to the intensity of action potential input (Araya, Eisenthal, & Yuste, 2006; Cash & Yuste, 1999; Jagadeesh, Wheat, & Ferster, 1993). These observations lead to the reformulated model in Figure 5B, establishing the relation between prestimulus EEG alpha power and stimulus-evoked P1 amplitude on a trial-by-trial basis, where an effective operational range *W* for the level of baseline activity can again be defined.

Experimental Test of Model Prediction

In our experiment, although the stimulus is kept constant, the background synaptic activity prior to stimulus onset, assessed by the amplitude of alpha oscillations, varies from trial to trial, leading to significant trial-to-trial variability in stimulus-evoked responses. Given the model in Figure 4, and its reformulation in terms of EEG variables in Figure 5, it is expected that the amplitude of the P1 component follows an inverted-U function of the prestimulus alpha power. This prediction is tested in Figure 6 for the attend condition. For each trial, the amplitude of the prestimulus (−300 to 0 msec) EEG activity in the frequency range of 8 to 12 Hz was estimated, rank-ordered from the smallest to the largest, and sorted into five equal-sized groups called power groups. The average normalized P1 amplitude in each prestimulus power group was plotted against the group index. Consistent with the model prediction, an inverted-U relation is clearly seen, implying that an intermediate level of alpha activity corresponds to highest levels of local gain and is most conducive to stimulus processing (Zhang & Ding, 2010). Individually, this relationship was robust across subjects, with the exception of Subject 2 and Subject 10, where a nonsystematic and a

negatively correlated relationship, respectively, were observed over the right parieto-occipital regions. Quantitatively, for the left occipital areas, when the subject was validly cued to the right visual field, the P1 amplitude for Power Group 3 (intermediate alpha power) is 63% and 104% higher than that for Power Group 1 (lowest alpha power) and Power Group 5 (highest alpha power) ($p = .0005$ and $p = .00025$, respectively, one-tailed paired Wilcoxon's signed-rank test). For the right occipital areas, when the subject is validly cued to the left visual field, the normalized P1 amplitude for Power Group 3 is 57% and 165% higher than that for Power Group 1 and Power Group 5 ($p = .02$ and $p = .0025$, respectively, one-tailed paired Wilcoxon's signed-rank test). Quadratic fits appear in Figure 6 as solid smooth curves to guide the eye.

Attentional Modulation of Baseline Ongoing Activity: A Possible Mechanism

Based on the model in Figures 4 and 5 and the results in Figure 6, it is plausible that brain circuits subserving covert attention, through top–down compensatory mechanisms, modulate the prestimulus ongoing neural activity to increase the overall slope of the sigmoidal function $O(S)$ in Figures 4 and 5, as illustrated in Figure 7A. This global change in the sigmoidal function, corresponding to an increase in global gain, can account for both reduced alpha power and enhanced P1 by attention (Figure 7A). Two predictions can be made according to Figure 7A. First, the attention-induced increase in local gain is not uniformly distributed over all possible levels of prestimulus EEG power. Specifically, the ratio between the two gain functions (attend vs. ignore) has again an inverted-U shape, as shown in Figure 7B. Second, the overall increase in the slope of the sigmoidal function is accompanied by a reduced effective operational range W, from $W1$ to $W2$, implying a reduction in the trial-to-trial variability of prestimulus alpha activity by attention to maximize stimulus-evoked response.

Test of Prediction 1

The data in Figure 6A and B, together with the data obtained in the same way from the ignore condition, are plotted in Figure 8A and B. It is evident that the gain, which reflects the slope of the sigmoidal function, is enhanced for the attend condition relative to the ignore condition. The ratios of the P1 amplitude between the two conditions for different prestimulus alpha power groups are shown in Figure 8C and D. As expected, the gain ratio is maximal for the intermediate power group, in agreement with the model prediction in Figure 7B. Quantitatively, for the left occipital areas, the P1 amplitude ratio for Power Group 3 (intermediate alpha power) is 52% and 68% higher than that for Power Group 1 (lowest alpha power) and Power Group 5 (highest alpha power). For the right occipital areas, the P1 amplitude ratio for Power Group 3 is 16% and 60% higher than that for Power Group 1 and Power Group 5. It is worth noting that the P1 component is relatively small for the ignore condition. Its subensemble estimation is further complicated by the fact that each power group in a given subject has only about 30 trials. These factors may explain the weak and sometimes even the lack of inverted-U appearance in Figure 8A and B, respectively, for the ignore condition.

Test of Prediction 2

Alpha band power in the interval −300 to 0 msec was estimated on a single-trial basis for each of the three conditions

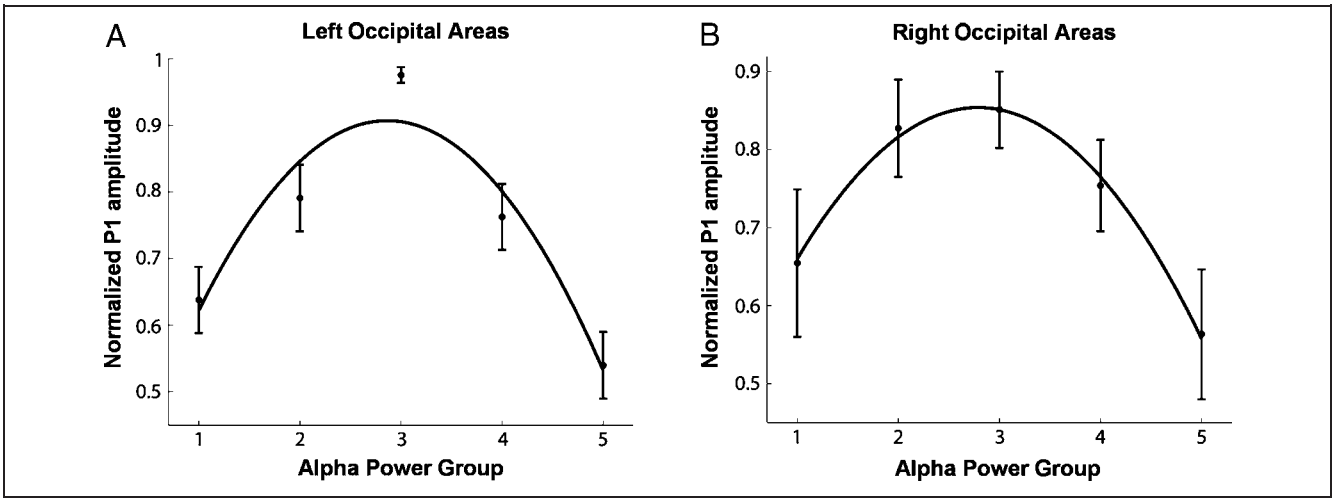

Figure 6. Relationship between prestimulus alpha power and stimulus processing. Trials with attended standard stimuli were considered (valid trials). Single trials were rank ordered by the magnitude of prestimulus alpha power (−300 to 0 msec) and sorted into five groups of equal size. The P1 component was determined for each group, normalized and averaged across subjects, and plotted as function of group index in (A) for left parieto-occipital areas and (B) for right parieto-occipital areas. An inverted-U relationship is clearly seen where the solid lines represent quadratic fits. Error bars are the standard error of the mean.

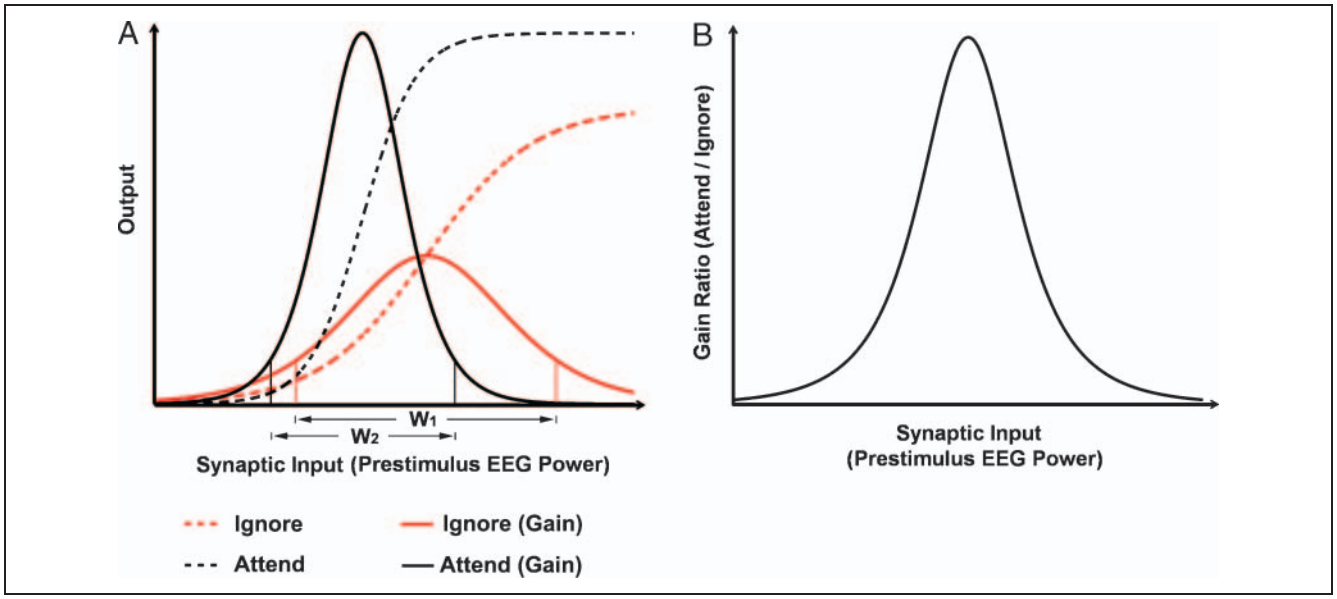

Figure 7. Schematic illustration of attentional modulation mechanisms of ongoing activity. (A) Attention shifts the sigmoidal curve in Figures 4 and 5 leftward and increases its overall slope (global gain). (B) The ratio of the gain curves in (A) for attend and ignore conditions is again an inverted-U function.

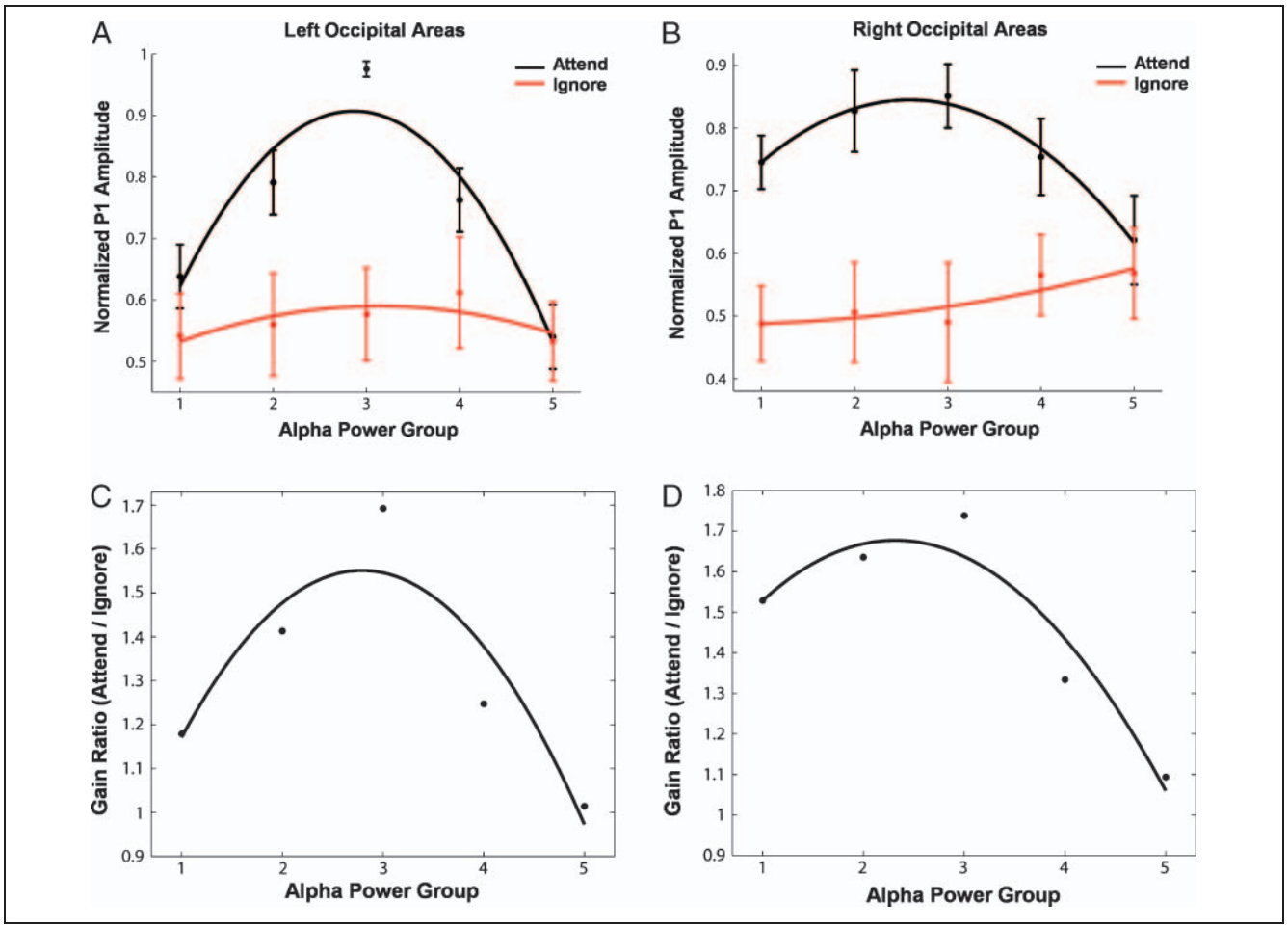

Figure 8. Gain ratio as a function of prestimulus alpha. P1 amplitude as a function of prestimulus alpha power is plotted for both attend and ignore conditions in (A) and (B). The ratios between the two curves are shown in (C) and (D). Maximum gain is achieved for intermediate levels of prestimulus alpha activity.

over the parieto-occipital sites and log-transformed. Figure 9A shows the Gaussian fits to the empirical distributions from a representative subject. The leftward shift of the distributions under task conditions corresponds to the reduced mean alpha power reported in Figure 3. In addition, both the attend and ignore conditions have narrower alpha power distributions relative to that of the fixation condition, with the distribution for the attend condition further narrowed from that for the ignore condition. Figure 9B summarizes the variance of the empirical alpha distribution across all subjects for the attend and ignore conditions. The variance reduction when attention is deployed to the contralateral visual field (attend) relative to the ipsilateral visual field (ignore) was significant at $p = .003$ over both hemispheres, and the reduction relative to the fixation condition was significant at $p = .0005$. The variance over the left hemisphere for the attend-right condition was significantly lower than that for the attend-left condition and for the fixation condition at $p = .00075$ and .0005, respectively. The variance over the right hemisphere for the attend-left condition was lower than that for the attend-right condition and for the fixation condition at $p = .088$ and .021, respectively. In addition, the variance for the ignore condition collapsed over both hemispheres is lower than that for the fixation condition at $p = .01$.

DISCUSSION

We considered the relation between visually evoked response and prestimulus alpha activity. Three results were found: (1) the P1 amplitude is shown to be an inverted-U function of the prestimulus alpha power (Figure 6), providing key evidence for the validity of the sigmoidal function model in Figures 4 and 5; (2) attentional enhancement of the P1 amplitude is interpreted as reflecting an increase in the overall slope of the sigmoidal function; and (3) in addition to amplitude reduction, the trial-to-trial variability of alpha is also reduced by attention, corresponding to a reduced working range as a consequence of the attentional modulation of the sigmoidal function (Figure 7). In light of these results, some of the seemingly conflicting observations in relation to alpha oscillations and stimulus processing may be reconsidered. First, in a given behavioral state (e.g., attend, ignore, or fixation), the inverted-U relation in Figures 5 and 6 indicates that intermediate levels of prestimulus alpha activity lead to strongest stimulus-evoked response. This may explain why both high and low levels of prestimulus alpha activity are not conducive to the detection of a threshold level stimulus (Romei, Brodbeck, et al., 2008; Romei, Rihs, et al., 2008; Babiloni et al., 2006; Ergenoglu et al., 2004). This explanation, together with reports in the somatosensory domain where the rate of detecting a weak stimulus is highest for intermediate levels of mu activity (Zhang & Ding, 2010; Linkenkaer-Hansen et al., 2004), appears to suggest a mechanism of sensory processing that is modality independent. Second, attentional reduction of alpha power, possibly mediated by top–down compensatory mechanisms (Capotosto, Babiloni, Romani, & Corbetta, 2009; Bressler, Tang, Sylvester, Shulman, & Corbetta, 2008), is taken to indicate the increased overall slope of the sigmoidal function, and thus, the higher global gain to input, and should not be extrapolated to imply that prestimulus alpha be inversely proportional to stimulus-evoked response.

Theoretical Consideration

The state of the brain fluctuates in a seemingly random manner. The fate of a sensory stimulus depends on the waxing and waning of the physiological variables characterizing these fluctuations (Lakatos, Karmos, Mehta, Ulbert, & Schroeder, 2008; Lakatos et al., 2005). Although the brain circuits mediating behavior, such as attention, modulates the global dynamics of these variables (Fischer, Langner, Birbaumer, & Brocke, 2008; Thut et al., 2006; Sauseng

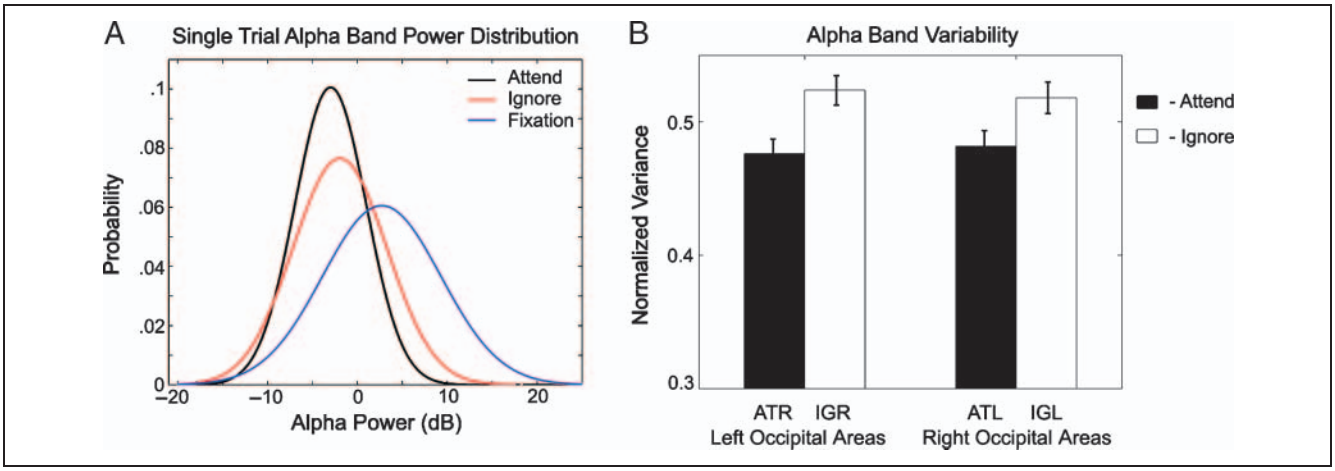

Figure 9. Distribution of alpha power. (A) Distributions of log-transformed single-trial alpha power for attend, ignore, and fixation conditions over left parieto-occipital areas from a representative subject. Variance of the single-trial alpha power distribution is compared over subjects between attend and ignore conditions in (B) where a reduction in variance is taken as evidence of decreased trial-to-trial alpha power variability.

et al., 2005; Foxe et al., 1998), on a given trial, the processing of a stimulus is affected by the magnitude of these variables immediately preceding its onset. In this work, the global state of a neuronal ensemble is assumed to be defined by a sigmoidal function, where the horizontal axis is the level of background synaptic activity over a suitably defined time interval and the vertical axis is the output firing rate over the same interval. On a trial-by-trial basis, the stimulus-evoked response is proportional to the derivative of the sigmoidal curve referred to as local gain, which is an inverted-U function of background synaptic activity level preceding the stimulus (Figure 4). Attention is hypothesized to enhance the global gain to sensory input by increasing the overall slope of the sigmoidal function. This model, while inspired by recent computational studies on the impact of mean and variance of membrane potential fluctuations on a neuron's responsiveness to input (Haider et al., 2007; Wolfart et al., 2005; McCormick et al., 2003; Chance et al., 2002; Ho & Destexhe, 2000), differs from these models in two important ways. First, the horizontal axis in Figure 4, rather than being the external input of varying intensity, is the level of moment-by-moment synaptic background activity assessable by dendritic field potentials. Second, an explicit mechanism is given, which stipulates that the stimulus-evoked response is an inverted-U function of the level of background synaptic activity immediately preceding stimulus onset.

Model Testing and Validation

In Figure 5, the model in Figure 4 is reformulated in which the amplitude of the P1 component is equated with the intensity of stimulus-evoked firing and the prestimulus alpha power with the level of background synaptic activity. A single-trial based analysis was carried out, and as predicted, an inverted-U relationship between the P1 amplitude and the prestimulus alpha power was found for both hemispheres (Figure 6). Considered a validation of the model, this finding suggests that the observed increase in P1 amplitude to the attended stimulus reflects increased global gain, which is defined by an increase in the overall slope of the sigmoidal function (Figures 7 and 8). The change in the sigmoidal function could further include a possible leftward shift of the sigmoidal function and a reduced effective operational range, both of which were confirmed by computing and comparing across experimental conditions the mean prestimulus alpha power (Figure 3) and the variance of the alpha power distribution (Figure 9). It is worth noting that qualitatively similar results were observed when alpha power was replaced by total signal variance to index background activity. The alpha activity was chosen as a proxy for the strength of background synaptic activity because (1) all subjects exhibited prominent spectral power in this band, accounting for most of the total signal variance, and (2) robust attentional modulation was observed in this band. In our data, attentional modulation in the other frequency bands, including theta, beta, and gamma, was either completely absent or was not statistically significant across subjects. In addition, power in higher-frequency bands such as beta and gamma are too small to serve as a representative variable for total synaptic background activity.

The prestimulus interval was chosen to be (−300 to 0 msec) in this study with 0 msec denoting the onset of the imperative stimulus. Our results were found to be robust for prestimulus intervals ranging from (−200 to 0 msec) to (−600 to 0 msec). However, longer prestimulus intervals such as those of 1 sec or longer in duration introduced increased variability across subjects, with some beginning to exhibit unsystematic relationships departing from the inverted-U function. This observation suggests that a long prestimulus interval, while yielding improved frequency resolution, may not provide an accurate characterization of the state of the brain at stimulus onset.

P1: Genesis and Attentional Modulation

The visually evoked P1 component reflects the early response of the extrastriate cortex and is enhanced by spatial attention (see Figure 2). Concerning its genesis, Mitzdorf (1985) showed in cats that a surface positive potential may arise due to excitatory synaptic activation of the supragranular pyramidal cells at their basal dendrites spanning layer 3 or portion of layer 4, which causes an extracellular sink near layer 4 and a superficial source composed of passive return current near the cortical surface. Similarly, in behaving macaques, Schroeder, Tenke, Givre, Arezzo, and Vaughan (1991) localized the primary generator of the pattern-evoked epidural P60, the monkey equivalent of the P1 in humans, to a current sink in layer 2/3, which was accompanied by an increase in unit firing and a current source along the apical dendrites of superficial pyramidal cells. The excitatory input to the superficial layers is considered to be from the layer 4 stellate cells, which receive afferent input from either thalamo-cortical projections or input from earlier sensory areas (Figure 5). According to these results, increased P1 amplitude by attention reflects increased firing of neuronal populations in layer 4, which is the basis for the choice of P1 for our analysis. The origins of the N1 and other later evoked components (Di Russo, Martinez, & Hillyard, 2003; Di Russo, Martinez, Sereno, Pitzalis, & Hillyard, 2002; Clark & Hillyard, 1996) are more complex. Their generation involves reentrant processing and the interaction among multiple brain areas (Garrido, Kilner, Kiebel, & Friston, 2007) and may depend, to a lesser extent, on prestimulus visual alpha. These components are thus not pursued here.

Alpha Oscillation: Neuronal Mechanisms and Attentional Modulation

The genesis of alpha oscillations in visual cortex is debated. Although early investigators focused on the pacemaking role of the thalamus, more recent work stresses

the cortical origin of the alpha oscillations. Bollimunta, Chen, Schroeder, and Ding (2008), analyzing laminar field potentials and multiunit activities from extrastriate cortical areas V2 and V4 of behaving macaques, found local generators of alpha in superficial layers, layer 4, and deep layers, and showed that the activities of these generators are highly synchronized. According to this view, the widely observed decrease of EEG alpha power with attention (Figure 3) likely reflects a similar decrease in the entire cortical column, allowing us to establish a link between scalp-measured alpha power and layer 4 neuronal firing, the latter being proportional to the magnitude of the P1 component.

Physiologically, the suppression of alpha is taken to imply increased cortical excitability (Jones, Pritchett, Stufflebeam, Hamalainen, & Moore, 2008; Romei, Brodbeck, et al., 2008; Romei, Rihs, et al., 2008; Klimesch, Sauseng, & Hanslmayr, 2007; Rihs, Michel, & Thut, 2007; Kelly, Lalor, Reilly, & Foxe, 2006; Thut et al., 2006; Sauseng et al., 2005; Goldman, Stern, Engel, & Cohen, 2002; Bastiaansen & Brunia, 2001; Marrufo et al., 2001; Jones, Pinto, Kaper, & Kopell, 2000; Worden, Foxe, Wang, & Simpson, 2000; Foxe et al., 1998). Cortical excitability is often understood in terms of mean depolarization levels of cellular membrane potentials and it does not have a simple linear relationship with stimulus-evoked response. For example, the absence or very low levels of spontaneous oscillatory activity may fail to bring local neuron populations closer to firing threshold, and excessive depolarization due to high levels of spontaneous activity may cause short-term synaptic depression, both of which can lead to diminished response to sensory input (Dehaene & Changeux, 2005; Petersen, Hahn, Mehta, Grinvald, & Sakmann, 2003; Chung, Li, & Nelson, 2002; Abbott, Varela, Sen, & Nelson, 1997). Although enhanced stimulus processing by attention in our experiment is thought to be mediated by increase in the slope of the sigmoidal function, as defined in Figure 7, excitability and gain in the current framework are not mutually exclusive concepts, and their symbiotic relationship was explored in a computational study presented in the Appendix (Figure 10). The

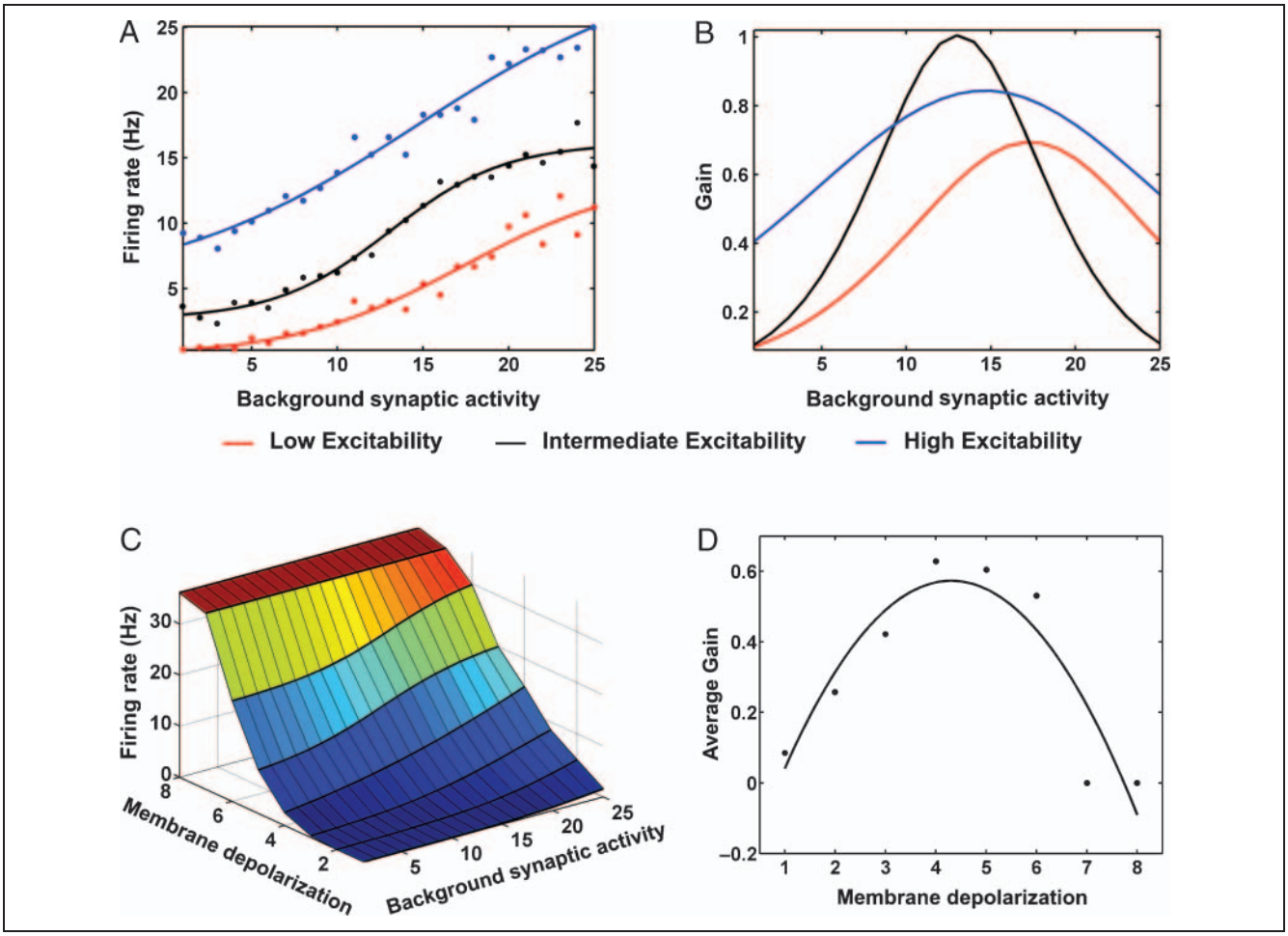

Figure 10. Computational study of relation between excitability and gain. (A) Firing rate over a 200-msec interval as function of background synaptic activity for three levels of mean membrane depolarization (blue: high excitability; black: intermediate excitability; and red: lower excitability). (B) Derivative of the sigmoidal curves in (A) showing nonlinear relationship between gain and background synaptic activity. (C) Firing rate as a function of mean membrane depolarization levels and variance of background synaptic activity. (D) Average gain, which corresponds to average stimulus-evoked response, for increasing levels of membrane depolarization.

results show that (1) there is an optimal range in mean membrane depolarization, which gives rise to highest overall slope of the sigmoidal function, and (2) both insufficient and excessive depolarization reduce the slope of the sigmoidal function, thereby reducing the response to sensory input. This computational study, together with the experimental data, suggests that (1) stimulus processing benefits directly from increased global gain and (2) attention optimally modulates excitability to enable such gain increase.

In addition to the amplitude, the phase of prestimulus alpha band oscillations can also significantly affect the magnitude of the evoked potential, and thus, stimulus processing (Klimesch, Sauseng, & Gruber, 2009; Mathewson, Gratton, Fabiani, Beck, & Ro, 2009; Lakatos et al., 2008; Makeig et al., 2002; Jansen & Brandt, 1991; also see Risner, Aura, Black, & Gawne, 2009; Ritter & Becker, 2009). When the stimulus occurrence is predictable, attention operates in the rhythmic mode (Schroeder & Lakatos, 2009), and an alignment of "high-excitability" phases of the oscillation with the attended events is considered a mechanism to enable enhanced sensory processing. In contrast, in the absence of a predictable temporal structure in the external stimuli, attention operates in the continuous mode (Schroeder & Lakatos, 2009), and the underlying neural ensemble is pushed into a continuous state of high excitability, indexed by sustained alpha magnitude suppression, to enable enhanced stimulus processing. The present experiment engages the continuous mode of attentional operation because the cue-imperative intervals were varied randomly over a wide range (1.8 to 2.2 sec), which rendered the imperative stimulus unpredictable. Furthermore, due to the random cue-imperative interval, the phase at stimulus onset within each power group is randomly distributed from 0 to 2π, ensuring that between different power groups, the phase is controlled, leaving the oscillation amplitude as the only independent variable.

APPENDIX

The relation between excitability and gain defined in Figures 4 and 7 was addressed computationally. The model (Destexhe et al., 2001) is composed of a single-compartment Hodgkin–Huxley type neuron with excitatory and inhibitory conductances representing the collective effect of a large number of synaptic inputs. The membrane potential is described by the following equation:

$$C\frac{dV}{dt} = -I_{Leak} - I_{Na} - I_{Kd} - I_M - \frac{1}{a}I_{syn} \qquad (1)$$

where $C = 1\ \mu F/cm^2$ is the specific membrane capacitance and $a = 34{,}636\ mm^2$ is the total membrane area of a typical cortical pyramidal cell. The five currents considered were: I_{Na} is the voltage-dependent Na^+ current, I_{Kd} the delayed rectifier K^+ current, I_M the non-inactivating K^+ current, I_{Leak} the leak current, and I_{syn} the synaptic current that has both an excitatory and an inhibitory component:

$$I_{syn} = g_e(t)(V - E_e) + g_i(t)(V - E_i) \qquad (2)$$

where $g_e(t)$ and $g_i(t)$ are time-dependent global excitatory and inhibitory conductances, respectively, with reversal potentials $E_e = 0$ mV and $E_i = -75$ mV. The synaptic conductances are assumed to be described by Ornstein–Uhlenbeck stochastic processes (Destexhe et al., 2001):

$$\frac{dg_e}{dt} = -\frac{1}{\tau_e}(g_e - g_{e0}) + \sqrt{\frac{2\sigma_e^2}{\tau_e}}x_e(t)$$
$$\frac{dg_i}{dt} = -\frac{1}{\tau_i}(g_i - g_{i0}) + \sqrt{\frac{2\sigma_i^2}{\tau_i}}x_i(t) \qquad (3)$$

where g_{e0} and g_{i0}, σ_e and σ_i, τ_e and τ_i are the average conductances, standard deviations, time constants for the excitatory and inhibitory inputs, respectively, and $x_e(t)$ and $x_i(t)$ are zero mean Gaussian white noise processes of unit standard deviation. The parameter values of Equation 3 were taken to be $\tau_e = 2.73$ msec and $\tau_i = 10.49$ msec, $g_{i0} = 0.06\ \mu S$, g_{e0} was varied between 0.01 and 0.0364 μS in steps of 0.0033, resulting in eight levels of increasing excitability. Twenty-five levels of background synaptic activity were simulated by changing the standard deviation of inhibitory conductance σ_i between 0 and 0.0375 μS in steps of 0.0015 μS. The parameter σ_e, the standard deviation for excitatory conductance, was kept constant at 0.006 μS. Qualitatively, similar results were obtained when σ_e was varied with σ_i kept constant or when both σ_i and σ_e were varied in tandem. Note that varying σ_i or σ_e also shares a correspondence with varying input correlation between individual synapses (Destexhe et al., 2001).

Forty trials each of 200 msec in duration were simulated for each of the 25 values of σ_i for eight excitability levels. Firing rate over the 200-msec interval was averaged across trials and plotted as a function of the variance of background synaptic activity in Figure 10A for three levels of excitability: low excitability (less depolarized, red curve), intermediate excitability (more depolarized, black curve), and high excitability (excessively depolarized, blue curve). The derivatives of all three sigmoidal functions are given in Figure 10B. Notice from Figure 10A and B that a moderate increase in depolarization increases gain, but too much excitability causes a decrease in gain. This nonlinear relation is further demonstrated by plotting the firing rate as a function of all eight levels of excitability and all 25 levels of variance of background synaptic activity in Figure 10C. The average stimulus-evoked response, defined as the weighted mean of the inverted-U function in Figure 10B, is plotted for each level of excitability in Figure 10D, which suggests the existence of an optimal range of excitability for enhanced stimulus processing.

Reprint requests should be sent to Mingzhou Ding, The J. Crayton Pruitt Family Department of Biomedical Engineering, University of Florida, Gainesville, FL 32611, or via e-mail: mding@bme.ufl.edu.

REFERENCES

Abbott, L. F., Varela, J. A., Sen, K., & Nelson, S. B. (1997). Synaptic depression and cortical gain control. *Science, 275,* 220–224.

Araya, R., Eisenthal, K. B., & Yuste, R. (2006). Dendritic spines linearize the summation of excitatory potentials. *Proceedings of the National Academy of Sciences, U.S.A., 103,* 18799–18804.

Babiloni, C., Vecchio, F., Bultrini, A., Romani, G. L., & Rossini, P. M. (2006). Pre- and poststimulus alpha rhythms are related to conscious visual perception: A high-resolution EEG study. *Cerebral Cortex, 16,* 1690–1700.

Bastiaansen, M. C. M., & Brunia, C. H. M. (2001). Anticipatory attention: An event-related desynchronization approach. *International Journal of Psychophysiology, 43,* 91–107.

Bollimunta, A., Chen, Y., Schroeder, C. E., & Ding, M. (2008). Neuronal mechanisms of cortical alpha oscillations in awake-behaving macaques. *Journal of Neuroscience, 28,* 9976–9988.

Brandt, M. E., & Jansen, B. H. (1991). The relationship between prestimulus alpha-amplitude and visual evoked-potential amplitude. *International Journal of Neuroscience, 61,* 261–268.

Brandt, M. E., Jansen, B. H., & Carbonari, J. P. (1991). Pre-stimulus spectral EEG patterns and the visual evoked-response. *Electroencephalography and Clinical Neurophysiology, 80,* 16–20.

Bressler, S. L., Tang, W., Sylvester, C. M., Shulman, G. L., & Corbetta, M. (2008). Top–down control of human visual cortex by frontal and parietal cortex in anticipatory visual spatial attention. *Journal of Neuroscience, 28,* 10056–10061.

Callaway, E. M. (1998). Local circuits in primary visual cortex of the macaque monkey. *Annual Review of Neuroscience, 21,* 47–74.

Capotosto, P., Babiloni, C., Romani, G. L., & Corbetta, M. (2009). Frontoparietal cortex controls spatial attention through modulation of anticipatory alpha rhythms. *Journal of Neuroscience, 29,* 5863–5872.

Cash, S., & Yuste, R. (1999). Linear summation of excitatory inputs by CA1 pyramidal neurons. *Neuron, 22,* 383–394.

Chance, F. S., Abbott, L. F., & Reyes, A. D. (2002). Gain modulation from background synaptic input. *Neuron, 35,* 773–782.

Chung, S., Li, X. R., & Nelson, S. B. (2002). Short-term depression at thalamocortical synapses contributes to rapid adaptation of cortical sensory responses in vivo. *Neuron, 34,* 437–446.

Clark, V. P., & Hillyard, S. A. (1996). Spatial selective attention affects early extrastriate but not striate components of the visual evoked potential. *Journal of Cognitive Neuroscience, 8,* 387–402.

Dehaene, S., & Changeux, J. P. (2005). Ongoing spontaneous activity controls access to consciousness: A neuronal model for inattentional blindness. *PLoS Biology, 3,* 910–927.

Destexhe, A., Rudolph, M., Fellous, J. M., & Sejnowski, T. J. (2001). Fluctuating synaptic conductances recreate in vivo-like activity in neocortical neurons. *Neuroscience, 107,* 13–24.

Di Russo, F., Martinez, A., & Hillyard, S. A. (2003). Source analysis of event-related cortical activity during visuo-spatial attention. *Cerebral Cortex, 13,* 486–499.

Di Russo, F., Martinez, A., Sereno, M. I., Pitzalis, S., & Hillyard, S. A. (2002). Cortical sources of the early components of the visual evoked potential. *Human Brain Mapping, 15,* 95–111.

Ergenoglu, T., Demiralp, T., Bayraktaroglu, Z., Ergen, M., Beydagi, H., & Uresin, Y. (2004). Alpha rhythm of the EEG modulates visual detection performance in humans. *Cognitive Brain Research, 20,* 376–383.

Ferree, T. (2006). Spherical splines and average referencing in scalp electroencephalography. *Brain Topography, 19,* 43–52.

Fischer, T., Langner, R., Birbaumer, N., & Brocke, B. (2008). Arousal and attention: Self-chosen stimulation optimizes cortical excitability and minimizes compensatory effort. *Journal of Cognitive Neuroscience, 20,* 1443–1453.

Foxe, J. J., Simpson, G. V., & Ahlfors, S. P. (1998). Parieto-occipital similar to 10 Hz activity reflects anticipatory state of visual attention mechanisms. *NeuroReport, 9,* 3929–3933.

Freeman, W. J. (1979). Non-linear gain mediating cortical stimulus–response relations. *Biological Cybernetics, 33,* 237–247.

Garrido, M. I., Kilner, J. M., Kiebel, S. J., & Friston, K. J. (2007). Evoked brain responses are generated by feedback loops. *Proceedings of the National Academy of Sciences, U.S.A., 104,* 20961–20966.

Gilbert, C. D., & Wiesel, T. N. (1983). Functional-organization of the visual-cortex. *Progress in Brain Research, 58,* 209–218.

Goldman, R. I., Stern, J. M., Engel, J., & Cohen, M. S. (2002). Simultaneous EEG and fMRI of the alpha rhythm. *NeuroReport, 13,* 2487–2492.

Haider, B., Duque, A., Hasenstaub, A. R., Yu, Y. G., & McCormick, D. A. (2007). Enhancement of visual responsiveness by spontaneous local network activity in vivo. *Journal of Neurophysiology, 97,* 4186–4202.

Hanslmayr, S., Aslan, A., Staudigl, T., Klimesch, W., Herrmann, C. S., & Bauml, K. H. (2007). Prestimulus oscillations predict visual perception performance between and within subjects. *Neuroimage, 37,* 1465–1473.

Hanslmayr, S., Klimesch, W., Sauseng, P., Gruber, W., Doppelmayr, M., Freunberger, R., et al. (2007). Alpha phase reset contributes to the generation of ERPs. *Cerebral Cortex, 17,* 1–8.

Heilman, K. M., Valenstein, E., & Watson, R. T. (2000). Neglect and related disorders. *Seminars in Neurology, 20,* 463–470.

Heinze, H. J., Mangun, G. R., Burchert, W., Hinrichs, H., Scholz, M., Munte, T. F., et al. (1994). Combined spatial and temporal imaging of brain activity during visual selective attention in humans. *Nature, 372,* 543–546.

Hillyard, S. A., Vogel, E. K., & Luck, S. J. (1998). Sensory gain control (amplification) as a mechanism of selective attention: Electrophysiological and neuroimaging evidence. *Philosophical Transactions of the Royal Society of London, Series B, Biological Sciences, 353,* 1257–1270.

Ho, N., & Destexhe, A. (2000). Synaptic background activity enhances the responsiveness of neocortical pyramidal neurons. *Journal of Neurophysiology, 84,* 1488–1496.

Jagadeesh, B., Wheat, H. S., & Ferster, D. (1993). Linearity of summation of synaptic potentials underlying direction selectivity in simple cells of the cat visual cortex. *Science, 262,* 1901–1904.

Jansen, B. H., & Brandt, M. E. (1991). The effect of the phase of prestimulus alpha activity on the averaged visual evoked response. *Electroencephalography and Clinical Neurophysiology, 80,* 241–250.

Jones, S. R., Pinto, D. J., Kaper, T. J., & Kopell, N. (2000). Alpha-frequency rhythms desynchronize over long cortical distances: A modeling study. *Journal of Computational Neuroscience, 9,* 271–291.

Jones, S. R., Pritchett, D. L., Stufflebeam, S. M., Hamalainen, M., & Moore, C. I. (2008). Influence of pre-stimulus somatosensory mu-rhythm on evoked response gain: A combined MEG and computational modeling study. *Society for Neuroscience Meeting Abstract*, 858.14.

Kelly, S. P., Lalor, E. C., Reilly, R. B., & Foxe, J. J. (2006). Increases in alpha oscillatory power reflect an active retinotopic mechanism for distracter suppression during sustained visuospatial attention. *Journal of Neurophysiology, 95,* 3844–3851.

Klimesch, W., Sauseng, P., & Gruber, W. (2009). The functional relevance of phase reset: A comment to Risner et al. (2009): The visual evoked potential of surface alpha rhythm phase. *Neuroimage, 47,* 5–7.

Klimesch, W., Sauseng, P., & Hanslmayr, S. (2007). EEG alpha oscillations: The inhibition-timing hypothesis. *Brain Research Reviews, 53,* 63–88.

Lakatos, P., Karmos, G., Mehta, A. D., Ulbert, I., & Schroeder, C. E. (2008). Entrainment of neuronal oscillations as a mechanism of attentional selection. *Science, 320,* 110–113.

Lakatos, P., Shah, A. S., Knuth, K. H., Ulbert, I., Karmos, G., & Schroeder, C. E. (2005). An oscillatory hierarchy controlling neuronal excitability and stimulus processing in the auditory cortex. *Journal of Neurophysiology, 94,* 1904–1911.

Linkenkaer-Hansen, K., Nikulin, V. V., Palva, S., Ilmoniemi, R. J., & Palva, J. M. (2004). Prestimulus oscillations enhance psychophysical performance in humans. *Journal of Neuroscience, 24,* 10186–10190.

Luck, S. J. (2005). *An introduction to the event-related potential technique*. Cambridge, MA: MIT Press.

Makeig, S., Westerfield, M., Jung, T. P., Enghoff, S., Townsend, J., Courchesne, E., et al. (2002). Dynamic brain sources of visual evoked responses. *Science, 295,* 690–694.

Mangun, G. R., Buonocore, M. H., Girelli, M., & Jha, A. P. (1998). ERP and fMRI measures of visual spatial selective attention. *Human Brain Mapping, 6,* 383–389.

Mangun, G. R., & Hillyard, S. A. (1991). Modulations of sensory-evoked brain potentials indicate changes in perceptual processing during visual spatial priming. *Journal of Experimental Psychology: Human Perception and Performance, 17,* 1057–1074.

Mangun, G. R., Hopfinger, J. B., Kussmaul, C. L., Fletcher, E. M., & Heinze, H. J. (1997). Covariations in ERP and PET measures of spatial selective attention in human extrastriate visual cortex. *Human Brain Mapping, 5,* 273–279.

Marrufo, M. V., Vaquero, E., Cardoso, M. J., & Gomez, C. M. (2001). Temporal evolution of alpha and beta bands during visual spatial attention. *Cognitive Brain Research, 12,* 315–320.

Mathewson, K. E., Gratton, G., Fabiani, M., Beck, D. M., & Ro, T. (2009). To see or not to see: Prestimulus phase predicts visual awareness. *Journal of Neuroscience, 29,* 2725–2732.

Mazaheri, A., & Jensen, O. (2006). Posterior alpha activity is not phase-reset by visual stimuli. *Proceedings of the National Academy of Sciences, U.S.A., 103,* 2948–2952.

McCormick, D. A., Shu, Y. S., Hasenstaub, A., Sanchez-Vives, M., Badoual, M., & Bal, T. (2003). Persistent cortical activity: Mechanisms of generation and effects on neuronal excitability. *Cerebral Cortex, 13,* 1219–1231.

Mitra, P. P., & Pesaran, B. (1999). Analysis of dynamic brain imaging data. *Biophysical Journal, 76,* 691–708.

Mitzdorf, U. (1985). Current source-density method and application in cat cerebral-cortex: Investigation of evoked-potentials and EEG phenomena. *Physiological Reviews, 65,* 37–100.

Niedermeyer, E., & Lopes da Silva, F. (1999). *Electroencephalography: Basic principles, clinical applications, and related fields* (4th ed.). Philadelphia, PA: Lippincott Williams and Wilkins.

Nunez, P. L., Srinivasan, R., Westdorp, A. F., Wijesinghe, R. S., Tucker, D. M., Silberstein, R. B., et al. (1997). EEG coherency: 1. Statistics, reference electrode, volume conduction, Laplacians, cortical imaging, and interpretation at multiple scales. *Electroencephalography and Clinical Neurophysiology, 103,* 499–515.

Paul, M. D., Simon, P. K., John, J. F., Richard, B. R., & Ian, H. R. (2007). Optimal sustained attention is linked to the spectral content of background EEG activity: Greater ongoing tonic alpha (approximately 10 Hz) power supports successful phasic goal activation. *European Journal of Neuroscience, 25,* 900–907.

Petersen, C. C. H., Hahn, T. T. G., Mehta, M., Grinvald, A., & Sakmann, B. (2003). Interaction of sensory responses with spontaneous depolarization in layer 2/3 barrel cortex. *Proceedings of the National Academy of Sciences, U.S.A., 100,* 13638–13643.

Rajagovindan, R., & Ding, M. (2008). Decomposing neural synchrony: Toward an explanation for near-zero phase-lag in cortical oscillatory networks. *PLoS ONE, 3,* e3649.

Rihs, T. A., Michel, C. M., & Thut, G. (2007). Mechanisms of selective inhibition in visual spatial attention are indexed by alpha-band EEG synchronization. *European Journal of Neuroscience, 25,* 603–610.

Risner, M., Aura, C., Black, J., & Gawne, T. (2009). The visual evoked potential is independent of surface alpha rhythm phase. *Neuroimage, 45,* 463–469.

Ritter, P., & Becker, R. (2009). Detecting alpha rhythm phase reset by phase sorting: Caveats to consider. *Neuroimage, 47,* 1–4.

Romei, V., Brodbeck, V., Michel, C., Amedi, A., Pascual-Leone, A., & Thut, G. (2007). Spontaneous fluctuations in posterior {alpha}-band EEG activity reflect variability in excitability of human visual areas. *Cerebral Cortex, 18,* 2010–2018.

Romei, V., Rihs, T., Brodbeck, V., & Thut, G. (2008). Resting electroencephalogram alpha-power over posterior sites indexes baseline visual cortex excitability. *NeuroReport, 19,* 203–208.

Sauseng, P., Klimesch, W., Stadler, W., Schabus, M., Doppelmayr, M., Hanslmayr, S., et al. (2005). A shift of visual spatial attention is selectively associated with human EEG alpha activity. *European Journal of Neuroscience, 22,* 2917–2926.

Schroeder, C. E., & Lakatos, P. (2009). Low-frequency neuronal oscillations as instruments of sensory selection. *Trends in Neurosciences, 32,* 918.

Schroeder, C. E., Tenke, C. E., Givre, S. J., Arezzo, J. C., & Vaughan, H. G. (1991). Striate cortical contribution to the surface-recorded pattern-reversal Vep in the alert monkey. *Vision Research, 31,* 1143–1157.

Thomson, A. M., & Lamy, C. (2007). Functional maps of neocortical local circuitry. *Frontiers in Neuroscience, 1,* 19–42.

Thomson, D. J. (1982). Spectrum estimation and harmonic analysis. *Proceedings of the IEEE, 70,* 1055–1096.

Thut, G., Nietzel, A., Brandt, S. A., & Pascual-Leone, A. (2006). Alpha-band electroencephalographic activity over occipital cortex indexes visuospatial attention bias and predicts visual target detection. *Journal of Neuroscience, 26,* 9494–9502.

Van Dijk, H., Schoffelen, J. M., Oostenveld, R., & Jensen, O. (2008). Prestimulus oscillatory activity in the alpha band predicts visual discrimination ability. *Journal of Neuroscience, 28,* 1816–1823.

Wolfart, J., Debay, D., Le Masson, G., Destexhe, A., & Bal, T. (2005). Synaptic background activity controls spike transfer from thalamus to cortex. *Nature Neuroscience, 8,* 1760–1767.

Worden, M. S., Foxe, J. J., Wang, N., & Simpson, G. V. (2000). Anticipatory biasing of visuospatial attention indexed by retinotopically specific alpha-band electroencephalography increases over occipital cortex. *Journal of Neuroscience, 20,* RC63.

Zhang, Y., & Ding, M. (2010). Detection of a weak somatosensory stimulus: Role of the prestimulus mu rhythm and its top–down modulation. *Journal of Cognitive Neuroscience, 22,* 307–322.

Zhang, Y., Wang, X., Bressler, S. L., Chen, Y. H., & Ding, M. Z. (2008). Prestimulus cortical activity is correlated with speed of visuomotor processing. *Journal of Cognitive Neuroscience, 20,* 1915–1925.